EFFECTS OF NICKEL SOURCE MATERIAL ON CHARACTERISTICS OF NICKEL/ALUMINA IMPREGNATED CATALYSTS

YOSHIMITSU UEMURA, YASUO HATATE AND ATSUSHI IKARI
Department of Chemical Engineering, Kagoshima University, Kagoshima 890

Key Words: Chemical Reaction, Nickel Alumina Catalyst, Nickel Particle Size, Nickel Source Material, Impregnation, Benzene Hydrogenation, X-ray Diffraction, Electron Probe Microanalysis, Transmission Electron Microscopy

A characterization study was undertaken with eighteen kinds of nickel/alumina impregnated catalysts prepared by using three nickel compounds (nickel (II) acetylacetonate, nickel (II) acetate and nickel (II) chloride) as the nickel source material and by applying two impregnation methods (single and multiple). The catalysts prepared by using nickel (II) acetylacetonate and nickel (II) acetate showed a similar distribution and average of nickel particle diameters regardless of nickel source material or impregnation method. The distribution broadening and the average increased with increasing nickel content for the catalysts prepared by using nickel (II) chloride. The rate of benzene hydrogenation was proportional to the nickel surface area regardless of nickel source material or impregnation method.

Introduction

Many supported catalysts in common use consist of small metal particles dispersed on a support having high surface area. Generally, these dispersions are produced by impregnating a support with a liquid in which the catalytic source material is dissolved. To control the performance of impregnated catalysts it is necessary to relate the physical properties and reactivity of the catalysts to the preparation conditions. Recently, many studies of impregnation have been undertaken: 1) the kinetics of metal ion transfer within porous support;[9,10,21] 2) the effects of support on characteristics of the catalysts;[3,11-13,16,18] 3) studies of post-impregnation drying condition;[7,17,18,20] 4) investigation of activation step.[4] No systematic study, however, has been made of the effects of catalytic source material on the physical properties and reactivity of the catalysts. Only a few investigations have been reported about the effects of platinum salt on platinum particle size,[2] XPS measurements of adsorbed nickel species on alumina from various nickel salts,[8] and the uptake of noble metal complexes with alumina.[15]

In previous studies, we investigated the effects of support nature,[18-20] support particle size,[17] metal content,[17,19] solvent of impregnant,[19] and post-impregnation drying condition[17,18,20] on the physical properties and reactivity of nickel/alumina impregnated catalysts. In this work, the characterization of nickel/alumina impregnated catalysts was investigated by using three nickel compounds (nickel (II) acetylacetonate, nickel (II) acetate and nickel (II) chloride) and by applying two impregnation methods (single and multiple).

Received April 24, 1987. Correspondence concerning this article should be addressed to Y. Uemura.

1. Experimental

1.1 Preparation of catalysts

1) Materials Three nickel compounds (nickel (II) acetylacetonate, nickel (II) acetate and nickel (II) chloride) were used as catalytic source materials. A sieved fraction from 48 to 100 mesh (average diameter 0.223 mm) of crushed high-surface area alumina (JRC-ALO-1 supplied by Catalysis Society of Japan) was used as a support. Typical properties of the support are given in **Table 1**.

2) Procedure The procedure and the conditions of catalyst preparation are summarized in **Fig. 1** and **Table 2**. The high-surface area alumina (average diameter 0.223 mm) was impregnated with the nickel compound solutions shown in Table 2 at room temperature for 3 h. The ratios of support to solution are given in Table 2. Besides single impregnation, multiple impregnation was also applied. The impregnated samples were dried by a rotary evaporator in three sequential stages (Fig. 1). Eighteen kinds of nickel/alumina impregnated catalysts (Table 2) were obtained by reducing about 0.05 kg of the dried samples in a stream of pure hydrogen gas at 200 $cm^3 \cdot min^{-1}$ and 723 K for 17 h.

1.2 Characterization of catalysts

1) Nickel content The nickel content of each catalyst was determined by titrating the nickel (II) ion in a sample solution prepared by dissolving the nickel of

Table 1. Physical properties of JRC-ALO-1

Form	White sphere
Composition	$\eta+\gamma$-alumina[6]
BET surface area [$m^2 \cdot kg^{-1}$]	1.69×10^5 [5]
Modal pore diameter [nm]	9.0[6]
Specific pore volume [$m^3 \cdot kg^{-1}$]	6.70×10^{-4} [6]

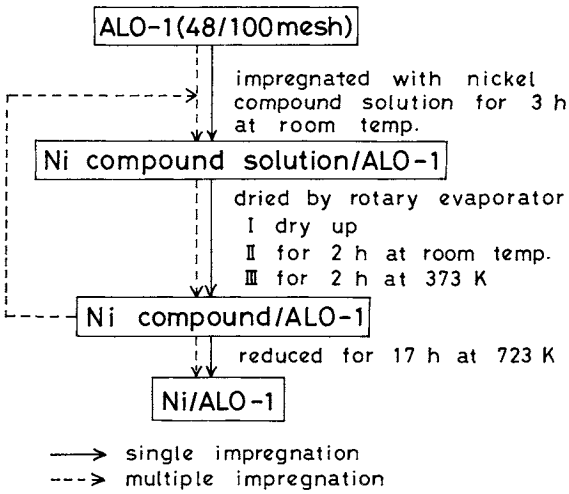

Fig. 1. Procedure of preparation of catalyst.

the catalyst in hydrochloric acid and filtering.

2) Intracatalyst nickel concentration profile Intracatalyst nickel concentration profiles were measured by electron probe microanalyser (EPMA, Shimadzu ARL microprobe X-ray analyser). The catalyst was imbedded in a thermoplastic resin. After solidification, sand paper (No. 220, 600, and 1500) was used to grind off the catalyst particles so as to expose the cross section. For fine polishing, No. 3000 sand paper was used. The sample was coated with a layer of carbon by vacuum deposition. The acceleration voltage of the electron beam was 15 kV and the sample current was 0.05 μA. The scanning speed was 0.02 mm $\cdot$ min^{-1}.

3) Morphology of nickel particles Transmission electron microscopy (TEM, Hitachi H-700H) was applied to determine the diameters of nickel particles and their distribution in the catalyst. Finely ground catalyst particles were suspended in distilled water and ultrasonically dispersed. Large particles were permitted to settle out, and a drop of the fine-particle suspension was placed on a collodion membrane and dried. Then, it was coated with a layer of carbon by vacuum deposition. About 100 nickel particles were measured for diameter inspection, using at least ten enlarged photographs of 200,000 X. The acceleration voltage of the electron beam was 500 kV and the filament current was 20 μA. Surface mean diameter ($\bar{D}_{p32}$) and volume mean diameter ($\bar{D}_{p43}$) were calculated from the following equations.

$$\bar{D}_{p32}=\frac{\Sigma D_p^3}{\Sigma D_p^2} \tag{1}$$

$$\bar{D}_{p43}=\frac{\Sigma D_p^4}{\Sigma D_p^3} \tag{2}$$

The line broadening of X-ray diffraction (XRD, Rigaku MJ 200DH) was applied to determine the volume mean diameter of nickel crystallite. XRD measurements were carried out by application of CuKα radiation with 40 kV of acceleration voltage and 30 mA of filament current. The volume mean diameter of nickel crystallite, $\bar{D}_{c43}$, was calculated from the following equations by using half-width of the (111) and (200) peaks.[1]

$$\bar{D}_{hkl}=\frac{0.9\lambda_{CuK\alpha}}{\beta_{1/2}\cos\theta} \tag{3}$$

$$\bar{D}_{c43}=\frac{\bar{D}_{111}+\bar{D}_{200}}{2} \tag{4}$$

1.3 Hydrogenation of benzene

Hydrogenation of benzene was used as a test reaction for the activity of the nickel/alumina catalysts. The reaction was carried out in an atmospheric flow system with a fixed-bed reactor made from Pyrex tube of 10 mm inner diameter.

About 100 mg of the catalyst (bed volume 0.15 cm^3) was packed into the reactor and was pretreated in a stream of hydrogen at 673 K for 1 h. After cooling down to reaction temperature (483 K), the reactant gases were allowed to flow through the catalyst bed. The partial pressure of benzene was 2.3 kPa and that of hydrogen was 70.9 kPa. The space velocity was about 40 s^{-1}. Reactor effluent samples were injected into a gas chromatograph via a microvolume sampling valve. Cyclohexene and cyclohexane were detected as reaction products. The reaction rate of the first step, benzene to cyclohexene, was calculated to study the catalytic activity.

2. Results and Discussion

2.1 Physical properties of catalysts

1) Intracatalyst nickel concentration profile The nickel concentration profiles were uniform regardless of nickel compound, the solvent of impregnant, or impregnation method. Typical results are illustrated in **Fig. 2**, which indicates that the effects of nickel content on the characteristics of the catalysts can be estimated correctly using the catalysts prepared in this study.

2) Morphology of nickel particles Transmission electron micrographs of ALO-1 and A1TA7-S are shown in **Fig. 3** as a representative example. The nickel particles are clearly visible as black circle-like images and the striations in each photograph are

Table 2. Catalysts prepared

Catalyst name	Impregnant	Impregnant/ support ratio [$l \cdot kg^{-1}$]	Impregnation (for 3 h at room temp.)	Nickel content [wt%]	Key	Group name
A1TA3-M	0.117M $Ni(AA)_2 \cdot 2H_2O$*	0.67 × 3	Multiple	1.28	●	TA-M
A1TA6-M	THF solution	0.67 × 6		2.74		
A1TA3-S		2.0		1.36		
A1TA4-S		2.7		1.89		
A1TA5-S	0.117M $Ni(AA)_2 \cdot 2H_2O$*	3.3	Single	2.24	○	TA-S
A1TA6-S	THF solution	4.0		2.66		
A1TA7-S		4.7		3.19		
A1TA10-S		6.8		4.47		
A1MA3-S		5.9		1.11		
A1MA5-S	0.040M $Ni(AA)_2 \cdot 2H_2O$* methanol solution	9.8	Single	2.11	▽	MA-S
A1MA10-S		19.4		4.28		
A1MS3-S		2.0		1.35		
A1MS5-S	0.114M $Ni(CH_3COO)_2 \cdot 4H_2O$	3.3	Single	2.20	△	MS-S
A1MS7-S	methanol solution	4.6		2.92		
A1MS10-S		6.7		4.29		
A1MC3-S	0.114M $NiCl_2 \cdot 6H_2O$	2.0	Single	1.39	◇	MC-S
A1MC7-S	methanol solution	4.7		2.94		
A1WC4-S	0.116M $NiCl_2 \cdot 6H_2O$ aq. solution	2.7	Single	1.62	□	WC-S

* Nickel(II) acetylacetonate.

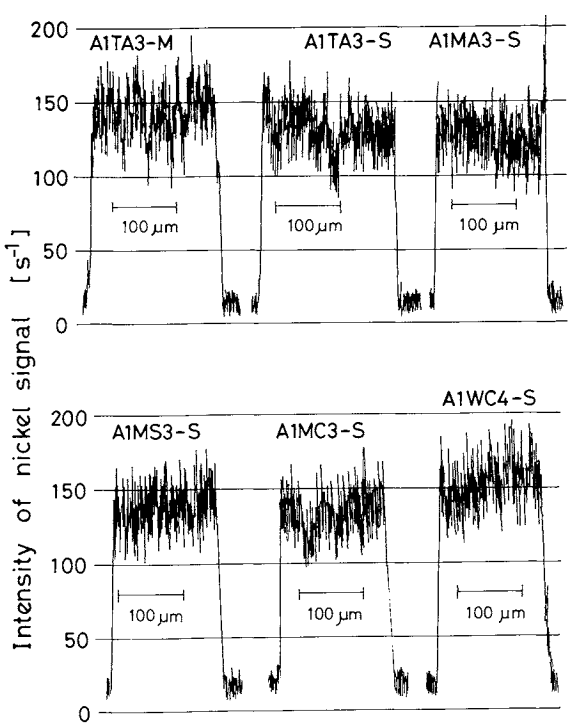

Fig. 2. Nickel response profiles of catalyst cross section by EPMA.

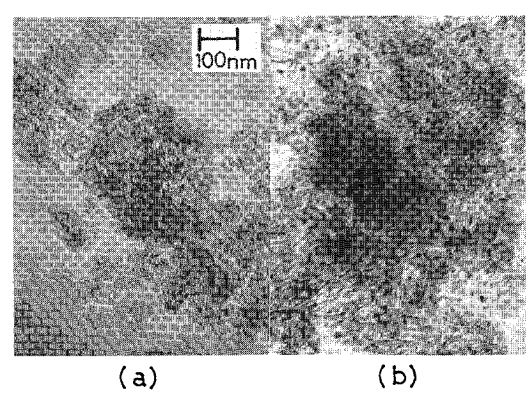

Fig. 3. Transmission electron micrographs of ALO-1(a) and AlTA7-S(b). (Black circle-like images represent nickel particles.)

referred to the support.

Figures 4 and **5** show the nickel particle size distributions of the catalysts prepared from THF solution of nickel (II) acetylacetonate (TA-S, Table 2) and from methanol or aqueous solution of nickel (II) chloride (MC-S and WC-S), respectively. The distributions of the other catalysts (TA-M, MA-S and MS-S) are similar to the result for TA-S (Fig. 4). The surface mean diameters of the nickel particles are plotted against nickel content in **Fig. 6**.

The similar distributions and averages among TA-M, TA-S and MA-S indicate that the number of repetitions of impregnation and the kinds of impregnant-solvents have no effect on the nickel particle size. The catalysts prepared from nickel (II) acetylacetonate and nickel (II) acetate show similar distributions and averages in the whole range of

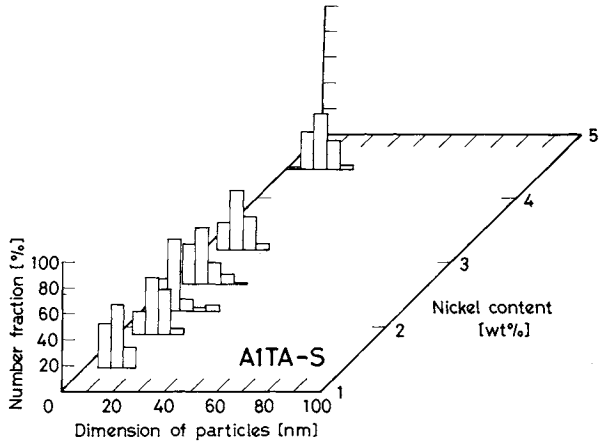

Fig. 4. Effects of nickel content on nickel particle size distributions of nickel/alumina catalysts (single impregnation with THF solution of nickel(II) acetylacetonate).

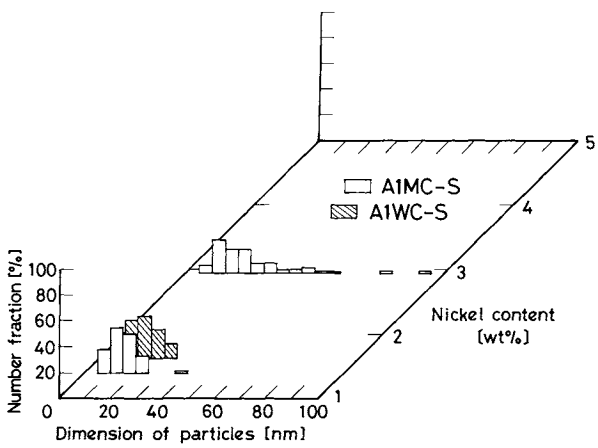

Fig. 5. Effects of nickel content on nickel particle size distributions of nickel/alumina catalysts (single impregnation with methanol or aqueous solution of nickel(II) chloride).

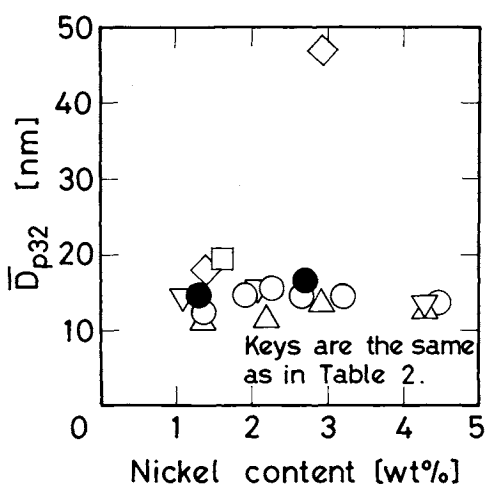

Fig. 6. Effects of nickel compound and impregnation method on average nickel particle diameter.

nickel content. On the other hand, the distribution broadening and average of nickel particle size in the catalysts from nickel (II) chloride increase with increasing nickel content as shown in Figs. 5 and 6. It is thought that the nickel particle growth occurs in the presence of volatile nickel chloride during the reduction step.[14]

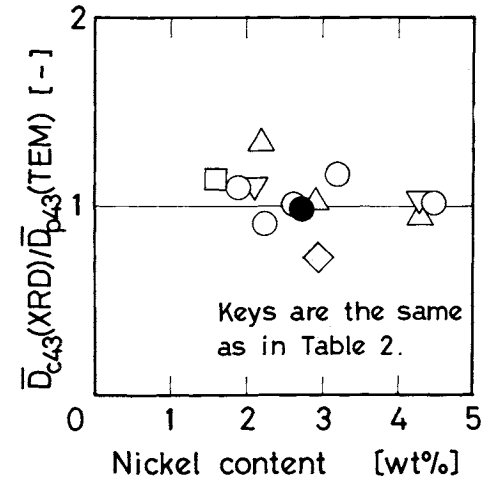

Fig. 7. Comparison of nickel crystallite diameter with nickel particle diameter.

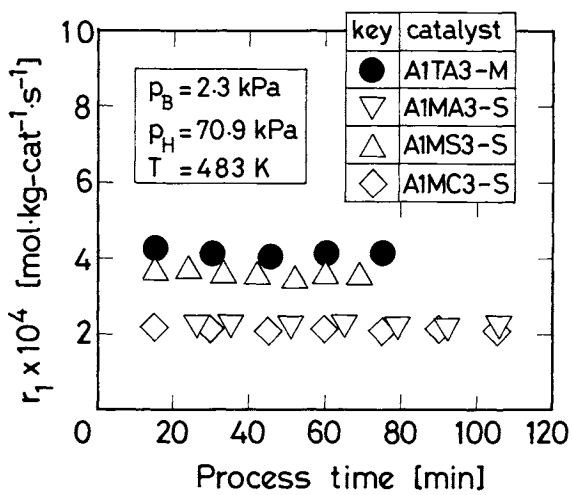

Fig. 8. Benzene hydrogenation rate as a function of process time.

In **Fig. 7**, the ratios of volume mean diameter of nickel crystallite to that of nickel particle are plotted against the nickel content. The fact that the mean crystallite diameter agrees with the mean particle diameter within $\pm 30\%$ shows that most nickel particles may consist of monocrystalline.

2.2 Hydrogenation of benzene

The hydrogenation rate did not change substantially with process time under the present conditions. Typical results are shown in **Fig. 8**.

Figure 9 shows the hydrogenation rate per unit mass of catalyst as a function of nickel surface area per unit mass of catalyst. The nickel surface area was calculated from the following equation.

$$S_{Ni} = 6 \times 10^7 \frac{w_t' f_R(w_t')}{\rho_{Ni} \bar{D}_{p32}} \tag{5}$$

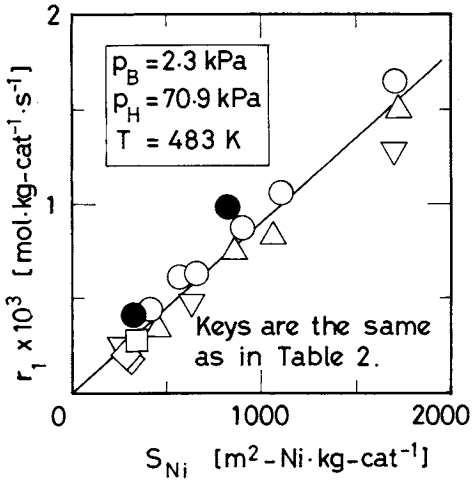

Fig. 9. Benzene hydrogenation rate as a function of nickel surface area.

Table 3. Applicable range of Eq. (6)

Support	JRC-ALO-1 JRC-ALO-3[19]
Impregnant solution	Nickel(II) acetylacetonate/THF Nickel(II) acetylacetonate/methanol Nickel(II) acetate/methanol Nickel(II) chloride/water Nickel(II) chloride/methanol Nickel(II) chloride/ethanol Nickel(II) chloride/1-propanol
Nickel content	From 1 to 8 wt%
Post-impregnation drying rate	From 2×10^{-6} to 2×10^{-3} kg-solvent·m^{-2}·s^{-1}
Reduction condition	Under flowing hydrogen gas at 723 K for 17 h.
Reaction condition	Partial pressure of benzene: 2.3 kPa Partial pressure of hydrogen: 70.9 kPa Tmperature: 483 K

The reduction degree of nickel, $f_R(w_t')$, was estimated from an empirical equation derived in the previous paper.[18] As shown in Fig. 9, there exists a linear relationship between the rate and the nickel surface area. That is, the rate is proportional to the nickel surface area regardless of nickel compound, solvent of impregnant, or impregnation method.

Since the linear relationship shown in Fig. 9 agrees with the previous results,[19] we obtain the following correlation between the hydrogenation rate and the nickel surface area in the wide range of the preparation conditions shown in **Table 3**.

$$r_1 = 9.0\times10^{-7} S_{Ni} \qquad (6)$$

Conclusion

Eighteen kinds of nickel/alumina catalysts were prepared by using three nickel compounds (nickel (II) acetylacetonate, nickel (II) acetate and nickel (II) chloride) and by applying two impregnation methods (single and multiple). Characterization of the catalysts led to the following conclusions.

1) The catalysts prepared from nickel (II) acetylacetonate and nickel (II) acetate show similar diameter distributions and average diameters of nickel particles in the whole range of nickel content (1–4 wt%), regardless of nickel source material or impregnation method. In the case of nickel (II) chloride, the distribution broadening and the average increase with increasing nickel content.

2) The hydrogenation rate of benzene is proportional to the nickel surface area regardless of nickel source material or impregnation method.

Acknowledgment

The authors wish to thank the Technical Research Laboratory of Kagoshima Prefecture for permitting us to use its X-ray diffractometer.

Nomenclature

D_p	=	diameter of nickel particle	[nm]
$\bar{D}_{c43}$	=	volume mean diameter of nickel crystallite	[nm]
$\bar{D}_{hkl}$	=	volume mean diameter of nickel crystallite perpendicular to *hkl* plane	[nm]
$\bar{D}_{p32}$	=	surface mean diameter of nickel particle	[nm]
$\bar{D}_{p43}$	=	volume mean diameter of nickel particle	[nm]
$f_R(w_t')$	=	reduction degree of nickel as a function of w_t'	[—]
p_B	=	partial pressure of benzene	[kPa]
p_H	=	partial pressure of hydrogen	[kPa]
r_1	=	hydrogenation rate from benzene to cyclohexene	[mol·kg-cat^{-1}·s^{-1}]
S_{Ni}	=	nickel surface area per unit mass of catalyst	[m^2-Ni·kg-cat^{-1}]
T	=	reaction temperature	[K]
w_t'	=	nickel content	[wt%]
$\beta_{1/2}$	=	half-width of XRD peak	[rad]
$\lambda_{CuK\alpha}$	=	X-ray wavelength (copper $K\alpha$)	[nm]
θ	=	Bragg angle	[rad]
ρ_{Ni}	=	density of nickel	[kg·m^{-3}]

Literature Cited

1) Anderson, J. R.: "Structure of Metallic Catalysts," p. 365, Academic Press (1975).
2) Baker, R. T. K., C. Thomas and R. S. Thomas: *J. Catal.*, **38**, 510 (1975).
3) Bartholomew, C. H. and C. K. Vance: *J. Catal.*, **91**, 78 (1985).
4) Bartholomew, C. H. and R. J. Farrauto: *J. Catal.*, **45**, 41 (1976).
5) Data-JRC-0001, Hattori, T.: *Shokubai* (*Chatalyst*), **22**, 115 (1980).
6) Data-JRC-0002, Mukaida, K.: *Shokubai* (*Catalyst*), **22**, 116 (1980).
7) Galiasso, R., O. L. de Ochoa and P. Andreu: *Appl. Catal.*, **5**, 309 (1983).
8) Gimzewski, J. K., B. D. Padalia and S. Affrossman: *J. Catal.*, **55**, 250 (1978).
9) Komiyama, H., T. Kataoka and H. Inoue: *Kagaku Kogaku Ronbunshu*, **10**, 337 (1984).
10) Komiyama, M., R. P. Merrill and H. F. Harnsberger: *J. Catal.*, **63**, 35 (1980).
11) Mustard, D. G. and C. H. Bartholomew: *J. Catal.*, **67**, 186 (1981).

12) Sannomiya, A., K. Ichimura, M. Yano and Y. Harano: *Kagaku Kogaku Ronbunshu*, **10**, 158 (1984).
13) Sannomiya, A., M. Yano and Y. Harano: *Kagaku Kogaku Ronbunshu*, **11**, 381 (1985).
14) Satterfield, C. N.: "Heterogeneous Catalysis in Practice," p. 137, McGraw-Hill (1980).
15) Summers, J. C. and S. A. Ausen: *J. Catal.*, **52**, 445 (1978).
16) Turlier, P., H. Praliaud, P. Moral, G. A. Martin and J. A. Dalmon: *Appl. Catal.*, **19**, 287 (1985).
17) Uemura, Y., Y. Hatate and A. Ikari: *J. Japan Petrol. Inst.*, **29**, 143 (1986).
18) Uemura, Y., Y. Hatate and A. Ikari: *J. Chem. Eng. Japan*, **19**, 560 (1986).
19) Uemura, Y., Y. Hatate and A. Ikari: *J. Japan Petrol. Inst.*, **30**, 53 (1987).
20) Uemura, Y., Y. Hatate and A. Ikari: *J. Chem. Eng. Japan*, **20**, 117 (1987).
21) Vincent, R. C. and R. P. Merrill: *J. Catal.*, **35**, 206 (1974).

HEAT TRANSFER COEFFICIENT IN THREE-PHASE VERTICAL UPFLOWS OF GAS-LIQUID-FINE SOLID PARTICLES SYSTEM

YASUO HATATE, SHUICHI TAJIRI, TAKANORI FUJITA, TAKASHI FUKUMOTO, ATSUSHI IKARI AND TADASHI HANO

Dept. of Chemical Engineering, Kagoshima Univ., Kagoshima 892

Key Words: Heat Transfer Coefficient, Three Phase Flow, Slurry Flow, Vertical Upflow, Solid Particle

Heat transfer characteristics between the inner tube wall and fluid of air-water-fine glass spheres three-phase vertical upflow were investigated using three kinds of glass spheres and two tubes under the following operating conditions:

gas velocity (U_G) = 80 – 900 cm/s, slurry velocity (U_L) = 30 – 160 cm/s, and solid particles concentration in slurry (C_S) = 5 – 54 wt% for D_T = 15-mm tube; and U_G = 15 – 305 cm/s, U_L = 8 – 62 cm/s, and C_S = 0.2 – 57 wt% for D_T = 27-mm tube.

The following results were obtained.

1) The heat transfer coefficients of three-phase vertical upflow exhibit larger values than those of gas-liquid two-phase vertical upflow in the range of 0–40 wt% solid concentration.

2) Monotonous small increases of the heat transfer coefficient with increase of both gas and slurry velocities were observed over the whole range of experimental conditions.

3) A new empirical correlation of heat transfer coefficient was proposed to fit all data obtained in this work within 30%.

Introduction

Reaction systems of gas-liquid-solid three-phase type have become of interest in recent years, since they have a wide variety of applications such as coal liquefaction, petroleum desulfurization and waste-water treatment. In the coal liquefaction process, pulverized coal is mixed with a solvent and hydrogen under high pressures of 100–200 atm in the preheater section and is then fed to the dissolver section to be liquefied.[1] It is especially important to understand the flow, heat transfer and mass transfer characteristics of three-phase flow with high fluid velocities in analyzing and designing the preheater section, in which slug flow is predominant.[1] In that section, temperature rises to about 450°C and the coal fed is almost dissolved to preasphaltenes. To develop an analysis of the preheater section, the flow characteristics in the vertical and horizontal tubes have been described in previous works[2,3] using air, water and fine glass spheres in place of hydrogen, solvent oil and coal particles, respectively. However, most studies of heat transfer in three-phase flow have been carried out under relatively mild conditions such as those in slurry bubble columns and three-phase fluidized beds. Little information is available for systems with the high fluid velocities that are predominant in some

Received December 25, 1986. Correspondence concerning this article should be addressed to Y. Hatate. T. Fujita is now at Daikin Co., Ltd., Osaka. T. Hano is at Dept. of Environmental Chemistry and Engineering, Oita Univ., Oita.